1-1-2015

A Comprehensive Design Approach for a MZM Based PAM-4 Silicon Photonic Transmitter

Kehan Zhu
Boise State University

Vishal Saxena
Boise State University

Xinyu Wu
Boise State University

A Comprehensive Design Approach for a MZM Based PAM-4 Silicon Photonic Transmitter

Kehan Zhu, Vishal Saxena, Xinyu Wu

Department of Electrical and Computer Engineering, Boise State University, Boise, ID 83725.

Email: kehanzhu@u.boisestate.edu

Abstract—A 4-level pulse amplitude modulation (PAM-4) silicon photonic transmitter targeting operation at 25 Gb/s is designed using an electrical-photonic co-design methodology. The prototype consists of an electrical circuit and a photonics circuit, which were designed in 130 nm IBM SiGe BiCMOS process and 130nm IME SOI CMOS process, respectively. Then the two parts will be interfaced via side-by-side wire bonding. The electrical die mainly includes a 12.5 GHz PLL, a full-rate 4-channel uncorrelated $2^7 - 1$ pseudo-random binary sequence (PRBS) generator and CML drivers. The photonics die is a 2-segment Mach-Zehnder modulator (MZM) silicon photonics device with thermal tuning feature for PAM-4. Verilog-A model for the MZM entails the system simulation for optical devices together with electrical circuitry using custom IC design tools. A full-rate 4-channel uncorrelated PRBS design using transition matrix method is detailed, in which any two of the 4-channels can be used for providing random binary sequence to drive the two segments of the MZM to generate the PAM-4 signal.

I. INTRODUCTION

Data bandwidth requirements in information and communication technology industry keep increasing exponentially as we transition into the era of 'Big Data'. This growth directly impacts the cost and the energy consumption of the network infrastructure. Silicon photonics technology, which can be used to fabricate optical devices using CMOS-compatible technology, not only brings integrated photonic chips into mass production but can also save significant amount of power to move 'big data' in the form of photons over $1000\times$ faster than in the form of electrons. Due to the advantages of enormous bandwidth, lower power consumption and interference immunity, silicon photonics is seen as the enabler for exponential data throughput growth at all levels of data communication hierarchy. This entails bringing low-cost photonic ICs into the racks in the future data centers, between chips on the mother board and backplanes, and even into future many-core processors.

Photonics community has successfully brought silicon photonics platform into a commercially accessible foundry service (e.g. IME in Singapore and ePIXfab from Europractice) but no process design kit (PDK) is available for simulation-based validation before chip fabrication. There are some commercial photonics device design tools in the market. However, the lack of interoperability with custom integrated circuits design tools makes electric-photonic co-design challenging. Also, new analog circuits are needed to leverage photonics to realize novel and optimized integrated solutions. We developed a mixed-signal electric-photonic co-design flow, which can simulate electrical circuits together with photonics devices as a system.

As a continuation of our previous work in [1] and [2], an integrated MZM based silicon photonics (pulse amplitude modulation) PAM-4 transmitter (TX) consists of an electrical die and a photonics die via side-by-side wire bonding which targets operation at 25 Gb/s is introduced. In [2] the PAM-4 MZM driver was systematically designed. However, it poses a practical testing problem that it needs two synchronized uncorrelated PRBS streams. Although test equipment vendors (e.g., Anritsu, Tektronix) provide pulse pattern generators (PPG) models which can provide multi-channel PRBS streams, their cost is prohibitive. And it's challenging to externally feed the input signals at such high speeds. Alternatively, multi-channel PRBS can be designed and fabricated on-chip. In this work, a system transition matrix design method is applied to design a full-rate 4-channel uncorrelated true $2^7 - 1$ PRBS generator, along with a complete MZM based PAM-4 TX architecture. MZM device modeling and bond wire parasitic modeling are addressed for the mixed signal simulation and design challenges. The rest of the paper is organized as follows. Section II illustrates the complete electrical chip architecture which is used to drive the MZM devices. Section III provides the PRBS design methodology and post-layout simulation results. Section IV discusses the system-level simulation and integration and Section V concludes the work with simulation results.

II. ARCHITECTURE OF THE ELECTRICAL CIRCUIT

The electrical driver IC reported in the latest MZM based silicon photonics PAM-4 TX literature [3] requires multi-channel 10 Gb/s PRBS externally feed into the chip which poses testing challenges. And photonics device community always like to use RF probes with bias-T and PPG to add electrical drive for their photonics device testing, like [4] realized a PAM-4 modulation with manipulating the magnitude and delay of two PRBS signals, then combined the two signals as an electrical PAM-4 signal before driving an MZM. However, this didn't leverage the benefits of processing high speed signals in the optical phase domain.

In Fig. 1, we proposed the system block diagram of the MZM driver architecture for the PAM-4 TX. The main blocks include a 12.5 GHz PLL, a 4-channel uncorrelated 2^7-1 PRBS and the PAM-4 driver. It has digital control tunability to compensate for the PVT variations. Explicit ESD protection devices are added for non high speed pads for reliability issue. With this proposed architecture, external high speed signals and clocks are thus avoided so that it will make the
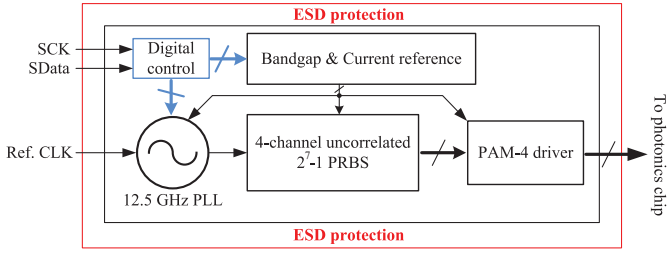
Fig. 1. System block diagram of the electrical driver for the MZM based PAM-4 TX.

system practical and the experimental characterization easy. PLL design and PAM-4 driver design were covered in [5] and [2], respectively, which will not be reiterated here. The PLL not only provides a clean 12.5 GHz clock for the PRBS, but also generates a 12.5/64 GHz synchronization clock for the sampling oscilloscope (Agilent 86100B) when measuring the eye diagram. The design of the 4-channel uncorrelated PRBS will be elaborated in the next section.

III. 4-CHANNEL UNCORRELATED 2^7-1 PRBS DESIGN

A half-rate 4-channel 23 Gb/s PRBS implemented with 8 DFFs was proposed in [6]. Only 7 of the DFFs were used in the feedback loops to generate 8 channels which were then multiplexed to obtain the 4-lane outputs. However, when using only 7 DFFs it is impossible to obtain four *uncorrelated* output streams with a period of 2^7 bits. Furthermore there is a redundancy in the feedback logic ($x^7 \oplus x^6 \oplus x^6 \oplus x^5 = x^7 \oplus x^5$) for the phase 315° DFF of Fig. 1 (b) in [6] (This is apparently because the authors of [6] did not apply modulo-2 addition when computing T^8, where T is the 7-by-7 transition matrix).

An n-stage linear feedback shift register (LFSR) PRBS generator is illustrated in Fig. 2. This topology can generate a PRBS of maximal length of $2^n - 1$ provided k is appropriately chosen. Some of the possibilities for n and k are given in the table in Fig. 2 [7].

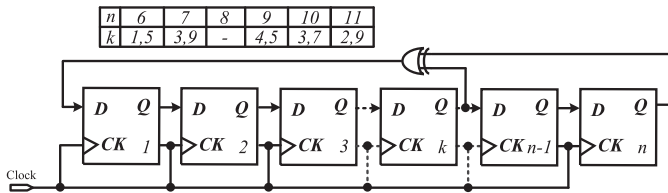| n	6	7	8	9	10	11
k	1,5	3,9	-	4,5	3,7	2,9

Fig. 2. An n-stage PRBS generator with possible n and k combinations (adapted from [7]).

In this design, $n = 9$ and $k = 5$ were chosen and the corresponding transition matrix T is given by (1). If the 9th DFF is initialized to 1 at the start and the others to 0, the initial state of the nine DFFs is then be presented as $s(0) = \begin{bmatrix} 0 & 0 & 0 & 0 & 0 & 0 & 0 & 0 & 1 \end{bmatrix}^T$. After l clock cycles, the state of the DFFs is $s(l) = T^l s(0)$.

$$T = \begin{bmatrix} 0 & 0 & 0 & 0 & 1 & 0 & 0 & 0 & 1 \\ 1 & 0 & 0 & 0 & 0 & 0 & 0 & 0 & 0 \\ 0 & 1 & 0 & 0 & 0 & 0 & 0 & 0 & 0 \\ 0 & 0 & 1 & 0 & 0 & 0 & 0 & 0 & 0 \\ 0 & 0 & 0 & 1 & 0 & 0 & 0 & 0 & 0 \\ 0 & 0 & 0 & 0 & 1 & 0 & 0 & 0 & 0 \\ 0 & 0 & 0 & 0 & 0 & 1 & 0 & 0 & 0 \\ 0 & 0 & 0 & 0 & 0 & 0 & 1 & 0 & 0 \\ 0 & 0 & 0 & 0 & 0 & 0 & 0 & 1 & 0 \end{bmatrix} \quad (1)$$

The output $s_9(j)$ of the above PRBS is either 1 or 0. In computing the correlation of sequences, it is standard practice to rescale the outputs to -1 and 1 respectively, which is done by letting $t(j) \triangleq 2s(j) - 1$. Implementing this transition matrix results in the sequence $\{t_9(j)\}=\{2s_9(j) - 1\}$ being uncorrelated with itself for a period of length 2^9 [7]. This implies that for $i = 0, 1, 2, ..., 2^9 - 1$, the auto-correlation is given by (2).

$$\phi(i) = \frac{1}{2^9 - 1} \sum_{j=0}^{2^9 - 1} t_9(j)t_9(j - i) = \begin{cases} 1, & i = 0 \\ \frac{-1}{2^9 - 1}, & i \neq 0 \end{cases} \quad (2)$$

As shown in [8], implementing T^4 (rather than T) results in the four outputs $s_5(l)$, $s_6(l)$, $s_7(l)$, $s_8(l)$ being uncorrelated with each other. These outputs are found using $s(l) = \left(T^4\right)^l s(0)$.

$$T^4 = \begin{bmatrix} 0 & 1 & 0 & 0 & 0 & 1 & 0 & 0 & 0 \\ 0 & 0 & 1 & 0 & 0 & 0 & 1 & 0 & 0 \\ 0 & 0 & 0 & 1 & 0 & 0 & 0 & 1 & 0 \\ 0 & 0 & 0 & 0 & 1 & 0 & 0 & 0 & 1 \\ 1 & 0 & 0 & 0 & 0 & 0 & 0 & 0 & 0 \\ 0 & 1 & 0 & 0 & 0 & 0 & 0 & 0 & 0 \\ 0 & 0 & 1 & 0 & 0 & 0 & 0 & 0 & 0 \\ 0 & 0 & 0 & 1 & 0 & 0 & 0 & 0 & 0 \\ 0 & 0 & 0 & 0 & 1 & 0 & 0 & 0 & 0 \end{bmatrix} \quad (3)$$

It then follows that $s_5(l)$, $s_6(l)$, $s_7(l)$, $s_8(l)$ are essentially uncorrelated for a period of 2^7. That is, with $t_p(j)=2s_p(j) - 1$ and $p = 5, 6, 7, 8$, for $i = 0, 1, 2, ..., 2^7 - 1$ that the cross-correlation is given by (4).

$$\phi_{pq}(i) \triangleq \frac{1}{2^7 - 1} \sum_{j=0}^{2^7 - 1} t_p(j)t_q(j - i) = \begin{cases} 1, & i = 0, \ q = p \\ \frac{-1}{2^7 - 1}, & i = 0, \ q \neq p \\ \frac{-1}{2^7 - 1}, & i \neq 0. \end{cases} \quad (4)$$

The PRBS generator was simulated with Spectre and the outputs were processed in Matlab to compute $\phi_{pq}(i)$ which is plotted in Fig. 4 over several periods of length 2^7 illustrating (4). The auto-correlation period of 2^9 for each output channel means that the single PRBS channel has a maximal length of 2^9-1. The uncorrelated length is reduced to 2^7-1 among the four selected channels. The corresponding block diagram for (3) with a schematic of XOR merged DFF are shown in Fig. 3. The four outputs $S1, \ldots, S4$ in Fig. 3 correspond to $s_5(l)$, $s_6(l)$, $s_7(l)$, $s_8(l)$. The first four rows of (3) show that the implementation requires 4 XORs. The fifth XOR in Fig. 3 is
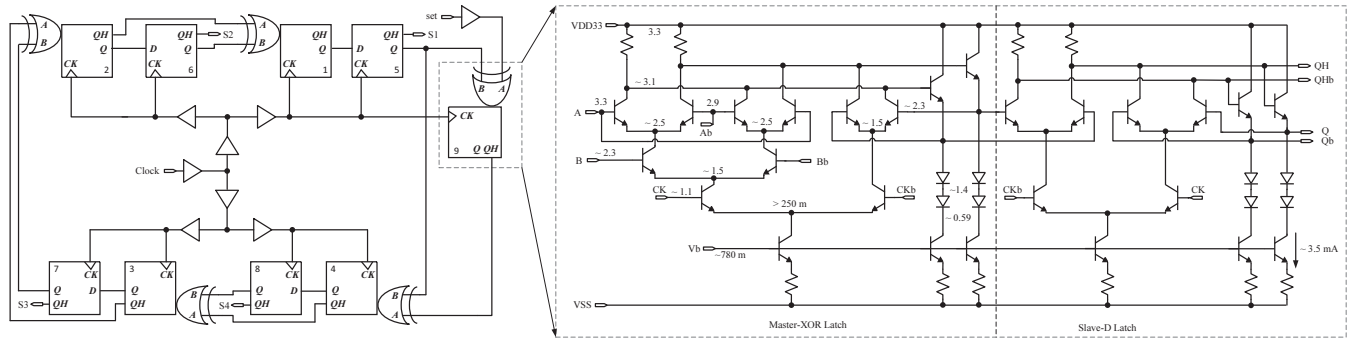
Fig. 3. Block diagram of the 4-channel $2^7 - 1$ uncorrelated PRBS (single-ended version, output buffers not shown); XOR merged DFF used in the PRBS generator (critical dc node voltages are annotated).

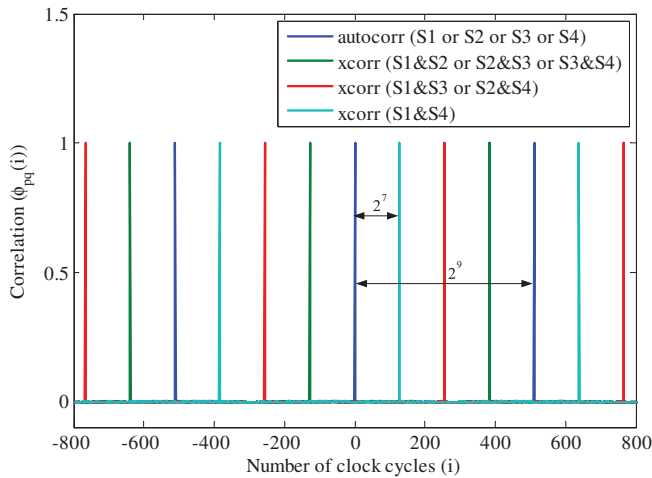used as a "set" signal to ensure the PRBS can start up from an all-zero state.

Fig. 4. Auto-correlation and cross-correlation of the 4-channel PRBS generator (signal amplitude rescaled to -1 and 1).
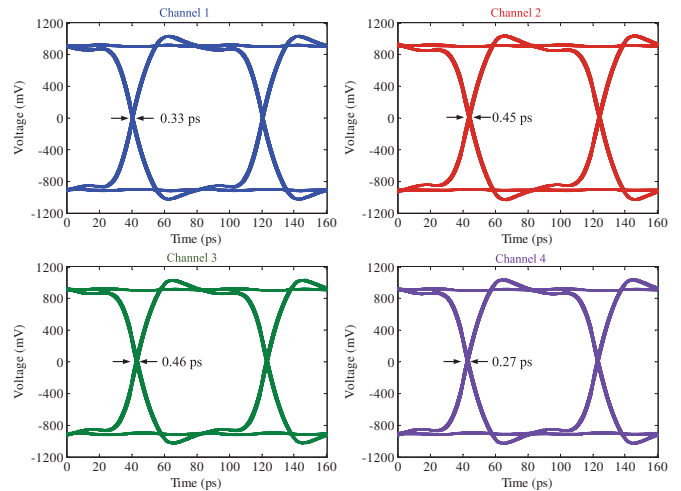

Fig. 5. Post-layout simulation results of eye diagram of 4-channel streams differential output data pattern at 12.5 Gb/s with a 12.5 GHz, 400 mV swing ideal sinusoidal input clock.

DFF, XOR logic and buffer are the three main circuit blocks used in the PRBS generator, which are all current mode logic (CML) topologies operating at very high speeds. A complete XOR-merged DFF [9] implemented using HBT BJT devices is shown in Fig. 3 along with the PRBS block diagram. It must be noted that the DFF in Fig. 3 has two output pairs (QH and QHb, Q and Qb). The QH and QHb output pair have higher common-mode voltage which are intended to drive the top devices (A and Ab input pair) in the XOR. Clock tree buffers and output buffers are critical and are CML with emitter follower based topology. The output buffers will output a signal swing of more than 800 mV to drive the CML driver designed in [2]. Fig. 5 plots the 4-channel differential outputs eye diagram from the post-layout simulation. It has a single-ened Vpp of more than 800 mV, maximum peak-to-peak jitter less than 0.48 ps when operating at 12.5 Gb/s. The power consumption is less than 1.4 W for the PRBS including clock tree and buffers circuits.

IV. SYSTEM-LEVEL SIMULATION AND INTEGRATION

Recent progress has been made with optical system-level design tools such as the Lumerical's Interconnect [10], which is specific to photonic integrated circuits (PIC) simulation and cannot be employed for hybrid optoelectronic system simulation, where a SPICE-like solver is required for transistor-level circuit simulations. Photonics device Verilog-A modeling and system-level integration issues will be addressed in this section.

A. MZM Device and Modeling

The imbalanced PAM-4 MZM device is made of two segments of phase shifters which are driven by two CML drivers as the layout top-view shown in Fig. 6. Coplanar waveguide (CPW) electrode is used for its low dispersion and more stable line impedance [11]. A thermal heater section is added for dc phase fine tune. The PAM-4 MZM acts like a 2-bit DAC which processes the signal in the optical phase domain. MZM model including voltage-dependent effective refractive index change, propagation delay, optical loss, thermo-optical coefficient and RLGC parameters can be described with Verilog-A [1], in which, the core element is the phase shifter as illustrated in Fig. 7. It shows the interaction between electric domain and photonics phase domain. For detailed modeling information, the readers are referred to our previous work in [1]
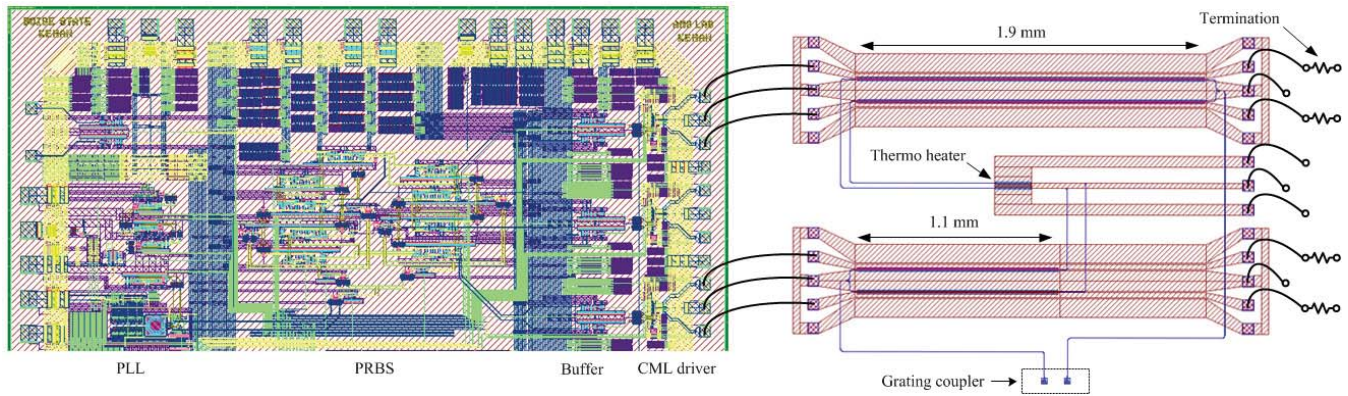
Fig. 6. System integration of electrical die (left) and photonics die (right) via side-by-side wire bonding (Bond wires drawn not to scale).
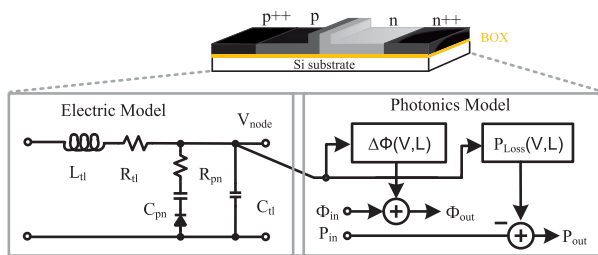

Fig. 7. Phase shifter model (device dimensions are drawn not to scale).

B. System Integration

A die-to-die wire bonding solution is illustrated in Fig. 6. Signal bond wires with a length of 2 mm (used for series inductive peaking) and a pitch of 200 μm (to avoid the cross coupling) proved to be necessary by putting the extracted S-parameters from ADS into Spectre simulation. Off-chip termination is planned at the far end of the MZM. Grating couplers will be aligned with fiber array to get the optical input and output. With an on-chip PLL and PRBS, all high frequency signals are avoided to be routed via PCB.
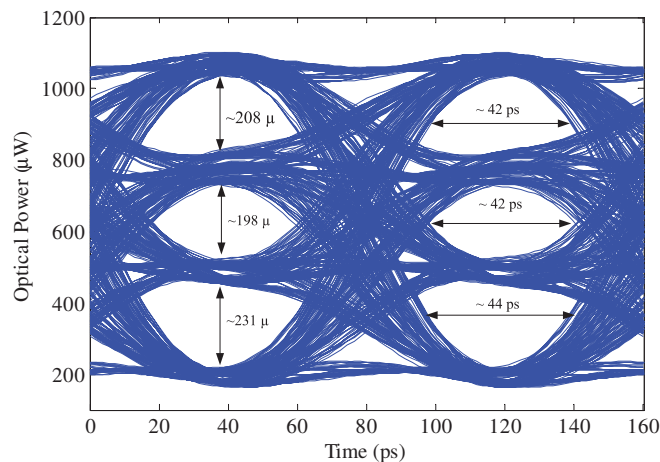

Fig. 8. Post-layout simulated optical output eye diagram of the complete TX circuits (excluding PLL) with PAM-4 MZM Verilog-A model at 25 Gb/s with a 12.5 GHz sinusoidal clock features a 0.5 V magnitude, a 7 ps peak-to-peak jitter to the PRBS .

V. CONCLUSION

An MZM based PAM-4 silicon photonics TX prototype was proposed for easy testing. A 4-channel uncorrelated $2^7 - 1$ PRBS generator design was systematically presented. Simulated optical eye as plotted in Fig. 8 was obtained with the hybrid simulation shows the TX can operate at 25 Gb/s.

ACKNOWLEDGMENT

REFERENCES

[1] K. Zhu, V. Saxena, and W. Kuang, "Compact Verilog-A modeling of silicon traveling-wave modulator for hybrid CMOS photonic circuit design," in *Proc. IEEE MWSCAS*, Aug 2014, pp. 615–618.

[2] K. Zhu, V. Saxena, X. Wu, and W. Kuang, "Design Considerations for Traveling-Wave Modulator Based CMOS Photonic Transmitters," *IEEE Trans. Circuits Syst. II, Exp. Briefs*, vol. 62, no. 4, pp. 412–416, April 2015.

[3] X. Wu, B. Dama, P. Gothoskar, P. Metz, K. Shastri, S. Sunder, J. Van der Spiegel, Y. Wang, M. Webster, and W. Wilson, "A 20Gb/s NRZ/PAM-4 1V transmitter in 40nm CMOS driving a Si-photonic modulator in 0.13 μm CMOS," in *Proc. IEEE ISSCC Dig. Tech. Papers*, Feb 2013, pp. 128–129.

[4] A. Samani, D. Patel, S. Ghosh, V. Veerasubramanian, Q. Zhong, W. Shi, and D. Plant, "OOK and PAM optical modulation using a single drive push pull silicon Mach-Zehnder modulator," in *Proceedings of IEEE 11th International Group IV Photonics*, Aug 2014, pp. 45–46.

[5] K. Zhu, V. Saxena, X. Wu, and S. Balagopal, "Design Analysis of a 12.5 GHz PLL in 130 nm SiGe BiCMOS Process," in *Microelectronics and Electron Devices (WMED), 2015 IEEE Workshop on*, March 2015, pp. 17–20.

[6] E. Laskin and S. Voinigescu, "A 60 mW per Lane, 4 x 23-Gb/s 2^7-1 PRBS Generator," *IEEE J. Solid-State Circuits*, vol. 41, no. 10, pp. 2198–2208, Oct 2006.

[7] H. M. Power and R. J. Simpson, *Introduction to dynamics and control*. McGraw-Hill UK, 1978.

[8] J. J. O'Reilly, "Series-parallel generation of m-sequences," *Radio and Electronic Engineer*, vol. 45, no. 4, pp. 171–176, April 1975.

[9] N. Mazumder, "Merging of logic function circuits to ECL latch or flip-flop circuit," Patent, Dec. 9, 1986, US Patent 4,628,216.

[10] "Lumerical Solutions, Inc. https://www.lumerical.com/." [Online]. Available: https://www.lumerical.com/

[11] N. I. Dib and L. P. Katehi, "Theoretical characterization of coplanar waveguide transmission lines and discontinuities." 1992.